Evidence for new regimes in channeled granular flows

Nicolas Brodu, Renaud Delannay, Alexandre Valance, and Patrick Richard
Institut Physique de Rennes, UMR CNRS 6251,
Université de Rennes 1, Campus de Beaulieu Bâtiment 11A,
263 av. Général Leclerc, 35042 Rennes CEDEX
(Dated: October 30, 2012)

By means of extensive numerical simulations, we discovered new regimes in channeled granular flows. These regimes emerge from the destabilization of unidirectional flows upon increase of mass holdup and inclination angle. They are characterized by non-trivial internal structures, with secondary flows and/or an heterogeneous mass distribution. The newly identified states include flows with a pair of rolls, superposed rolls, a basal ordered layer topped by secondary flows, and states where a dense core is supported by a gaseous phase. Besides, the supported regimes exhibit striking behaviors at high mass holdup such as symmetry breaking leading to periodic oscillations of the dense core. Interestingly, these different regimes are shown to obey a universal scaling law for the mass flow rate as a function of the mass hold-up. These new states provide a unique set of 3D flow regimes on which granular rheological models can be tested and open perspectives for interpreting geophysical granular flows.

PACS numbers: 47.57.Gc, 45.70.-n

arXiv:1210.7478v1 [cond-mat.soft] 28 Oct 2012

Introduction– Granular flows are encountered in many geophysical flows and industrial processes but there is still no general theoretical description for these flows. Progress has been made for flows down inclines [1–3] and current theories give a reasonable description for unidirectional and uniform flowing states. These simple flows have been shown to be unstable at large inclination angles and to develop longitudinal vortices [4, 5]. However, little is known about the instabilities of these unidirectional flows. One objective reason for this is that the parameter space accessible to experiments and simulations is restricted to a reduced domain compared to what is possible in nature. For example, the experimental observations of steady and fully developed flows at high angle and high mass flow rate would require long channels. We have developed optimized discrete element method (DEM) simulations that allow exploration of granular flows in wide channels at high inclination angles.

We consider a simple flow geometry with flat frictional basal and lateral walls. This geometry has been already used in previous experimental [6] and numerical [7] works and includes a wide variety of industrial or geophysical flows. Our numerical simulations reveal the existence of a rich variety of new regimes never reported in the literature. These new regimes emerge from the destabilization of steady and fully developed unidirectional flows upon increase of the mass holdup and the slope. They exhibit non-trivial internal structure with secondary flows and heterogeneous mass distribution, including states with array of rolls, a pair of rolls atop a basal sheared ordered layer, and dense cores supported by a gaseous phase. These new flow regimes are expected to be encountered in many real situations and raise a new challenge for extending the scope of current rheological models [2].

Method– We have performed 3D simulations of granular flows with a classical discrete element model [1, 8, 9]. This technique consists in integrating the equations of motion of all grains, and resolving their interactions by considering them as soft interpenetrating spheres. Details about this method can be found in our previous work [7]. The material parameters were chosen to match the experiments of Louge and Keast [6]: grain density $\rho_g = 2.5 \times 10^3 \text{kg/m}^3$, grain diameter $D = 3\,mm$, coefficient of restitution $e = 0.972$, grain/grain friction coefficient $\mu_g = 0.33$ and grain/wall friction $\mu_m = 0.59$. We used the same channel geometry as that employed by Louge and Keast in their experiments [6]. The channel has a rectangular section and a width $W \approx 68D$. We explicitly account for the presence of lateral walls,

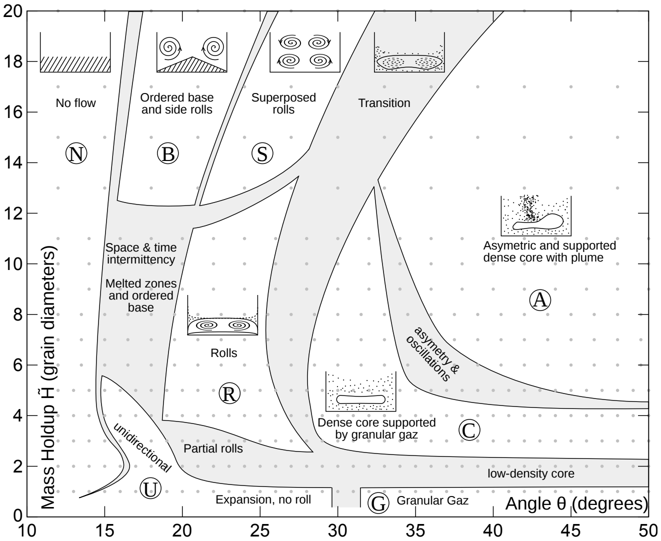

Figure 1: Granular flows down inclined channels phase diagram. Circled letters are used throughout this document to identify the regimes. Each of the 385 gray dots represents the result of a simulation that has reached its final state.

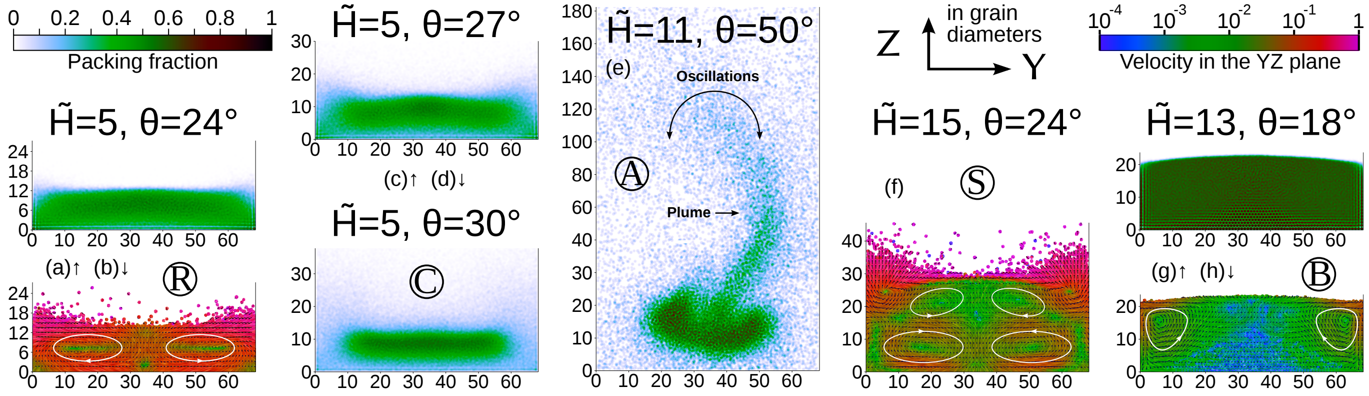

Figure 2: (Color online). Snapshots of different regimes. Packing fraction (a) and velocity field (b) in the transverse plane for the rolls regime Ⓡ. Packing fraction for the transition (c) to the supported symmetric dense core (d) regime Ⓒ. Packing fraction for the supported regime at high mass holdup Ⓐ, presenting an oscillating asymmetry (e). (f) Average velocity field in the transverse plane showing stacked rolls Ⓢ at high mass holdups. Average packing fraction (g) and velocity (h) in the transverse plane, presenting rolls in a "melted" zone on top of a base consisting of sheared ordered layers Ⓑ.

unlike most numerical studies considering periodic conditions in the flow transverse direction. Walls are not only physically relevant, but necessary in order to reach steady flows at high angles θ in simulations. They are sufficiently far away to allow for the development of secondary flows, which would not appear in more confined setups. Simulations were started with densely packed grains dropped at a small altitude from the basal wall and were run up to reaching a steady regime, possibly oscillatory.

We have varied the angle of inclination θ and the amount of matter per unit surface measured via the mass holdup $\tilde{H}$ defined as: $\tilde{H} = \frac{1}{D}\int_{z=0}^{\infty} \nu(z)dz$, where ν is the particle volume fraction. $\tilde{H}$ is the dimensionless height that the flow would have without voids between grains.

Phase Diagram– Qualitatively distinct regimes are identified according to the values of the inclination angle and mass holdup (see Fig. 1 and 2). Larger figures and snapshots are available in the supplementary materials. Fig. 1 indicates in the parameter space $(\theta, \tilde{H})$ the domain of existence of the different identified regimes. These are labeled by circled letters and are briefly described below:

– Regime Ⓤ corresponds to Unidirectional flows with sheared ordered layers of grains. The properties of these flows match the experimental observations reported by Louge and Keast [6] as detailed in [7].

– Regime Ⓡ corresponds to the presence of secondary Rolls, visible in Fig. 2b. These structures were previously reported and analyzed in recent experimental and numerical works [4, 5, 7]. In particular, an analogy with Rayleigh-Bénard convection rolls in heated liquid layers can be made, where the "granular temperature" plays the same role as the classical thermodynamics temperature [4]. Rolls break at larger angles θ when the flow lifts up on top of a layer of granular gas (regime Ⓒ), as illustrated in Fig. 2d.

– Regime Ⓒ is characterized by the presence of a dense Core floating on top of a granular gaseous phase. It is clearly visible on the density map of Fig. 2d. This regime is referred to as a supported flow. The core slowly "evaporates" as the angle increases for a gradual transition to granular gas at larger angles (shown in the supplementary materials). When the mass holdup increases, the core starts to swing back and forth from left to right and loses its axial symmetry.

– Regime Ⓐ denotes the Asymmetric core. For larger $\tilde{H}$ and θ, a "plume" forms on top of the core, as shown in Fig. 2e. This structure oscillates from one side to the other through time, recovering the symmetry on average.

– Regime Ⓢ corresponds to the Superposed rolls and appears at larger mass holdups $\tilde{H}$ than regime Ⓡ. An example is shown in Fig. 2f.

– Regime Ⓑ is characterized by the presence of a basal layered structure. The observed order (see Fig. 2g) is dynamically maintained by collisions and cage effects. The layers are sheared and not static. Rolls are present in the disordered zone on the top of the basal layers and are localized close to the lateral walls (Fig. 2h). This complex flow regime that exhibits both order/disorder transition and secondary flows raises a significant challenge for theoretical modeling.

These different flow regimes open many perspectives given the generality of the inclined channel geometry. The regimes Ⓤ and Ⓡ have been analyzed extensively in our preceding work [7]. Here, we focus on the supported regimes and present further details below.

Supported regimes– These regimes are of great interest because they may explain part of why low friction is observed for long run-out landslides. Campbell [10] indeed suggested that the existence of a layer of highly agitated particles at low concentration beneath a densely packed main body could reduce the apparent basal friction. By employing 2D [11] and 3D [12] discrete particles numerical simulations, it has been shown that a granular material subjected to gravity approaches this state if its initial kinetic energy is large enough. All these flows are in general not steady but decelerate or accelerate depending on the slope. Taberlet et al [12] simulated flows on bumpy inclined with lateral periodic boundary conditions, but these supported flows reach a steady regime only for a unique value of the slope. In our case, steady supported flows are obtained in a large range of inclination angles. This regime is very stable and robust to variations of the model parameters.

Fig. 3 shows typical density profiles for the supported regimes. Regimes Ⓐ and Ⓒ both present a dense core floating above a granular gaseous phase (Fig. 2d,e), and toped by a dilute "atmosphere". It is possible to see the signature of the "plume" (regime A) in the profiles above the core. The center of mass of the flow is located just on top of the core, so a large fraction of the matter is spread in the dilute atmosphere over large distance.

When the mass holdup increases the core lifts up and densifies, as shown in Fig. 3a. The lateral width of the core (see Fig. 2d,e) decreases with $\tilde{H}$ because the lateral pressure pushes the grains toward the central core. This core can reach very high values of the volume fraction up to 0.6 at large mass holdup, while the density in the supporting basal gaseous layer is below 0.2. The volume fraction in the dilute atmosphere above the core is well fitted by a decreasing exponential: $\nu(z) \propto \exp(-z/H_C)$, where H_C represents the characteristic height of the atmosphere (see the supplementary materials).

Surprisingly, when the angle θ increases, the average altitude of the core remains constant (see Fig. 3b). However, the center of mass lifts up and the core thickness decreases as a non-negligible part of the material is transferred into the top granular gaseous phase. Fig. 4a shows that for the supported regimes (indicated by dots in the Figure), the position C_M of the center of mass increases linearly with $\tan\theta$: $C_M = a\tan\theta + b$, where the slope a is independent of the mass holdup. In contrast, the parameter b increases with increasing mass holdup and reflects the corresponding increase of the core thickness with $\tilde{H}$ described in Fig. 3a.

The vertical expansion of the flow is necessary to increase its friction on the lateral boundaries and to balance the driving force which increases with the inclination angle. The basal friction cannot exceed $\mu_m M g\cos\theta$, where $\mu_m = 0.59$ is the microscopic friction value used in the simulations [7] and M is the mass of the grains. Thus for large angles, a large part of the friction comes from the lateral walls. The apparent friction coefficients on the base μ_b and walls μ_w are computed as the ratio of tangential to normal stresses averaged over all simulated impacts. Fig. 4b shows the dependency of μ_b on θ and $\tilde{H}$. μ_w follows the same trend up to very minor variations (see inset of Fig. 4b). Both coefficients increase and saturate at high inclination angles. In contrast, they decrease with the mass holdup: for a given angle, the basal friction reduces as more matter is added in the flow. This effect is reminiscent of what is observed for large natural flows in long run-out avalanches [10].

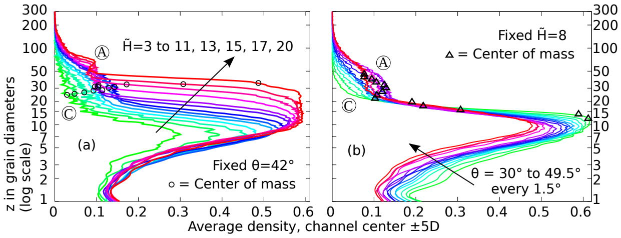

Figure 3: (Color online). Vertical profiles of the density of the flow at the center of the channel, averaged over 10D. (a) for a fixed angle $\theta = 42°$ when varying the mass holdup, and (b) for a fixed mass holdup $\tilde{H}$=8 when varying the angle. Empty dots and triangles indicate the position of the center of mass.

Using a force balance on the periodic cell in the stationary regime, we write: $Mg\sin\theta = 2\mu_w L\int_0^\infty N_w(z)dz + \mu_b N_b W L$, with $N_w(z)$ and N_b the normal stress at sidewalls and at the base respectively. $L = 20D$ is the length of the cell in the flow direction. The first term is the friction of the wall on the flow, and the second the friction of the base. We assumed Coulomb's friction as both μ_w and μ_b saturate in the supported regimes (Fig. 4b). The force balance in the other direction gives: $Mg\cos\theta = N_b W L$. This simple model thus predicts: $2\int_0^\infty N_w(z)dz/N_b = \frac{W}{\mu_w}(\tan\theta - \mu_b)$. The first term represents a characteristic height of the flow and will be denoted by H_p (if the pressure were purely hydrostatic, H_p would correspond exactly to the height of the flow). This relation expresses the fact that the characteristic height of the flow H_p varies linearly with $\tan\theta$. This explains why the position C_M of the center of mass, which is of the order of the half height of the flow, evolves linearly with $\tan\theta$. Remarkably, we find here a slope $a = 54.6 \approx W/(2\mu_m)$ in agreement with the hypothesis that $C_M \approx H_p/2$. We also find that the "atmospheric height" H_C increases linearly with $\tan\theta$ in the supported regimes. The slope here is about two third of W/μ_w, corresponding to $H_c \approx 3H_p/2$.

Transient– The typical temporal evolution of the average flow velocity to reach the steady regime is shown in Fig. 5a for $\tilde{H} = 5$. The data can be fitted with good accuracy (RMS error less than 6%) by an exponential saturation toward the limit velocity: $V(t) = V_L - (V_L - V_0)\exp(-t/\tau)$, where V_0 is the initial average velocity in the flow direction, V_L the limit velocity and τ a characteristic time. The adaptation of the flow during the transient requires a strong reorganization of its structure. Outstandingly, in spite of this, we observe a very regular evolution, with a similar behavior (exponential saturation) for all the angles, and thus for all the

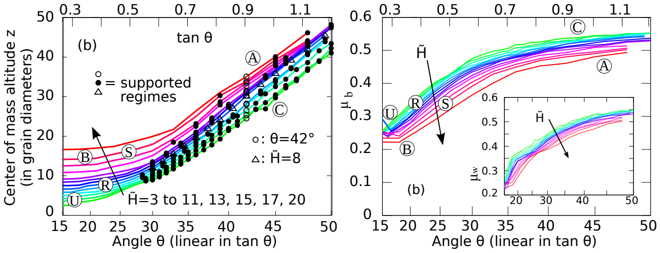

Figure 4: (Color online). (a) The center of mass C_M altitude, with respect to the slope angle θ. Markers indicate the configurations in the supported regimes Ⓐ and Ⓒ and (b) effective friction coefficients on the base μ_b and the wall (μ_w, inset), as defined in the main text.

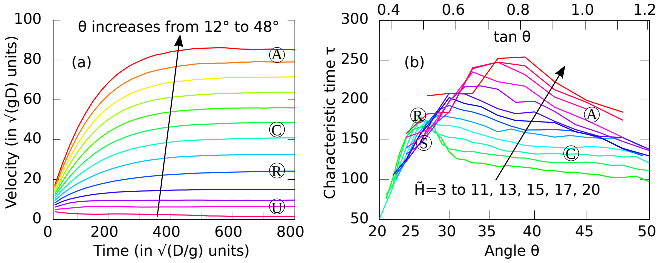

Figure 5: (Color online). (a) Typical temporal evolution of the mean flow velocity, for $\tilde{H} = 5$ and $\theta = 12°$ to $\theta = 48°$ every 3°. (b) Characteristic time for the flow to reach the limit velocity (small angles and intermittent states not shown).

regimes. On the other hand, the characteristic time τ is affected by changes of the inclination angle θ and the mass holdup $\tilde{H}$, as can be seen in Fig. 5b, which reveals a general tendency for longer transients in the roll regimes Ⓡ and Ⓢ in comparison with supported regimes Ⓒ and Ⓐ at larger angles.

The exponential velocity saturation suggests that the flow experiences a viscous-like drag force proportional to the velocity: $F_v = -MV/\tau$. Such a viscous frictional force due to collisions of grains with boundaries was already reported a long time ago [13]. The viscous damping constant $\alpha = M/\tau$ follows the inverse trend of τ, and increases with the mass holdup (shown in the supplementary materials). α is large for the regimes where grain interactions are dominated by collisions: Ⓤ and Ⓑ where collisions maintain dynamically the order, and supported regimes Ⓒ and Ⓐ lubricated by a highly collisional basal gaseous layer.

Steady state velocity– In contrast with the complex dependency of the relaxation time τ on θ and $\tilde{H}$, we identify a simple universal dependency for the limit velocity: $V_L/\tilde{H}^{1/4} \approx A \sin\theta + B$, where A and B are constant coefficients. In Fig. 6, we plotted the limit velocity V_L rescaled by $\tilde{H}^{1/4}$ as a function of the inclination angle θ for various mass holdup. A remarkable collapse is observed, given the large diversity of the flow regimes. In steady state, the mass flow rate is simply given by $Q = V_L\tilde{H}$. Our results thus show that $Q \propto \tilde{H}^{5/4}$ for a fixed angle θ, which is close to the scaling law ($Q \propto \tilde{H}^{3/2}$) derived by Louge and Keast from experiments [6] but obtained over a smaller range of flow rate Q.

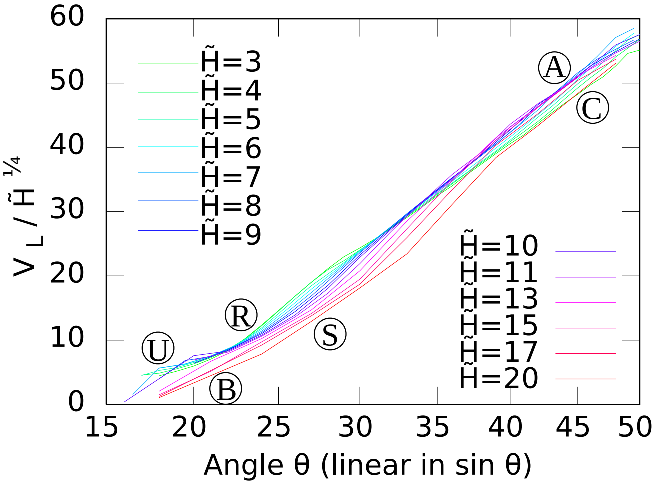

Figure 6: (Color online). Scaling law for the steady state velocity: $V_L/\tilde{H}^{1/4} \approx A\sin\theta + B$, with $A \approx 122$ and $B \approx -37$. The collapse is not perfect, but nonetheless remarkable given the diversity of regimes.

Conclusion– We explore granular flows configurations that were not previously attained in experimental or numerical works, with wide channels and large inclination angles. Using a simple flow configuration with flat lateral and basal boundaries, we have discovered, by varying the inclination angle and mass holdup, a multitude of new regimes ranging from rolls to dense cores supported by a highly agitated granular gaseous phase. These regimes present non-trivial features including heterogenous density, secondary flows, anisotropy, symmetry breaking, and dynamically maintained order.

For increasing angles, the flow inflates to balance the growing driving force by a larger friction on the lateral walls. At some stage the bulk of material lifts up to ride on a thin layer of agitated grains (supported regimes). For increasing mass holdup $\tilde{H}$, the lateral and basal effective friction coefficients reduce, revealing properties similar to long run-out avalanches in nature. Besides, we showed that the mass flow rate of these flows obeys a universal scaling law in terms of $\tilde{H}$. The new identified states provide a unique set of granular flow regimes for testing 3D rheological models and making further progress in the modeling of granular flows. These results also open new perspectives for understanding geophysical flows and should encourage investigations of granular flows in wider channels and for higher mass holdup.

Acknowledgements– This work was partly financed by the RISC-E RTR of the Université Européenne de Bretagne. We thank Michel Louge for helpful discussions and comments on our work.

[1] L E. Silbert, D. Ertas, G. S. Grest, T. C. Halsey, D. Levine, and S. J. Plimpton. *Phys. Rev. E*, 64:051302, 2001.

[2] GDR-MiDi. *Eur. Phys. J. E*, 14(4):341–365, aug 2004.

[3] R. Delannay, M. Louge, P. Richard, N. Taberlet, and A. Valance. *Nat. Mat.*, 6:99–108, 2007.

[4] Y. Forterre and O. Pouliquen. *J. Fluid Mech.*, 467:361–387, 2002.

[5] T. Börzsönyi, R. E. Ecke, and J. N. McElwaine. *Phys. Rev. Lett.*, 103:178302, 2009.

[6] M. Y. Louge and S. C. Keast. *Phys. Fluids*, 13(5):1213–1233, 2001.

[7] N. Brodu, P. Richard, and R. Delannay. Submitted to Phys. Rev. E, 2012.

[8] P.A. Cundall and O.D.L. Strack. *Géotechnique*, 29:47–65, 1979.

[9] S. Luding. *Eur. J. Env. Civil Eng.*, 12(7-8):785–826, 2008.

[10] C. S. Campbell. *J. of Geology*, 97(6):653–665, 1989.

[11] P. W. Cleary and C. S. Campbell. *J. Geophys. Res.*, 98:21911, 1993.

[12] N. Taberlet, P. Richard, J. T. Jenkins, and R. Delannay. *Euro. Phys. J. E: Soft Mat. Bio. Phys.*, 22(1), 2007.

[13] G. G. Batrouni, S. Dippel, and L. Samson. *Phys. Rev. E*, 53:6496, 1996.